

Preparation and Photoactivity of the Immobilized TiO₂/chitosan Layer

Jérôme Le Cunff^{a,b}, Vesna Tomašić^b, Zoran Gomzi^b

^aXellia d.o.o., Slavenska avenija 24/6, 10000 Zagreb, Croatia

^bUniversity of Zagreb, Faculty of Chemical Engineering and Technology, Trg Marka Marulića 19, 10000, Zagreb, Croatia
jerome.le-cunff@xellia.com

Heterogeneous photocatalytic oxidation processes employing semiconducting oxides such as TiO₂, ZnO, etc. and appropriate irradiation sources have demonstrated promising results for the degradation of many persistent organic pollutants, producing more biologically degradable and less toxic substances. Recent advances in photocatalysis have focused on improving current photoreactor performance to make the process economically feasible. The immobilization of the photocatalyst in the form of a thin film significantly reduces some of the drawbacks of practical application of heterogeneous photocatalysis with nanoparticles. The photolytic and photocatalytic activity was investigated in the photocatalytic batch annular reactor system with recirculation, using different sources of irradiation. Terbutylazine (N-tert-butyl-6-chloro-N'-ethyl-1,3,5-triazine-2,4-diamine), a substitute for atrazine, was used as model pollutant. The influence of various operating conditions on degradation of terbutylazine was investigated and obtained results are discussed. The Langmuir-Hinshelwood (L-H) mechanistic model is employed to describe the overall reaction rate. The results obtained in this study have shown that the delicate balance between excellent mechanical properties of the woven roving glass fibers and satisfactory adhesion of the photocatalytic layer, have important role in preparation of the functional modular photocatalyst easily placed inside the photoreactor. Apparently, the modelling of the photoreactor to optimize its performance will be crucial from the perspective of efficient design and the application of the heterogeneous photocatalytic degradation of herbicides in wastewater.

1. Introduction

Modern industrial progress has generated a vast range of toxic, non-biodegradable compounds of synthetic nature, such as pharmaceuticals, personal care products, dyes as well as pest control compounds used in agricultural sector. These compounds can be present in the surrounding soil, leachate and wastewaters (Wilson and Tisdell, 2001) but their removal using conventional wastewater treatment has proven to be expensive and ineffective (Ormad et al., 2008). Photocatalytic oxidation (PCO) proved to be suitable method for purification of waters, especially for very toxic compounds present in small concentrations in wastewater. TiO₂ is the most investigated and used photocatalyst, with main features, such as availability, great catalytic activity and non-toxicity, especially if used in heterogeneous catalysis (Ayati et al., 2014). Although most of the research was performed on suspended particles, the development of thin immobilized photocatalytic layers is becoming more interesting due to the problems with photocatalysis using suspended nanoparticles (Ghimici and Nichifor, 2013). A smaller specific surface and the increased difficulties to irradiate the entire available surface with the optimal light intensity is the new issue, but the photocatalyst applied on a surface can be more easily modified, the reactor design can also contribute to overall efficiency, especially taking regeneration into count (Mozia et al., 2012). The materials and chemicals used in this study needed to be cost effective, environmentally friendly. The P25 titanium dioxide is the most researched and applied semiconductor photocatalyst on the market due to its excellent properties (Herrmann, 2010). Chitosan is a material with wide biomedical and agricultural applications produced from a natural and readily available polymer similar to cellulose, chitin (Dash et al., 2011).

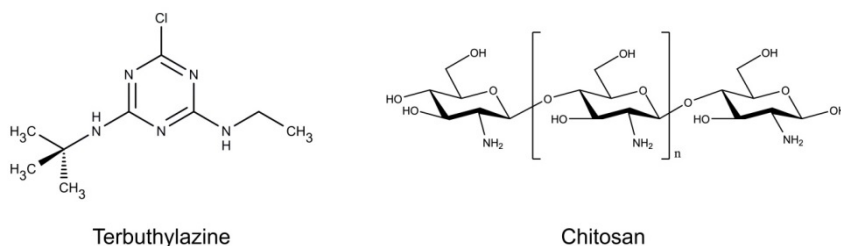


Figure 1. Schematic representation of structure of terbutylazine (*N*-tert-butyl-6-chloro-*N'*-ethyl-1,3,5-triazine-2,4-diamine) and chitosan ($[\beta$ -(1-4)-2-amino-2-deoxy-D-glucose]).

Glass fibre woven roving materials are already extensively used for many industrial applications, usually to increase the stiffness and strength of fiberglass materials. It is a robust material resistant to biological and chemical degradation and often used in very harsh environments, and has excellent binding properties with chitosan (Dwight, 2000). Photolytic and photocatalytic degradation of the model component terbutylazine was investigated in the photocatalytic batch annular reactor system with recirculation, using different sources of irradiation, placed in the central part of the photoreactor. The influence of various operating conditions (temperature, pH, recirculation flow, radiation intensity and wavelength, aeration flow) on the photolytic and photocatalytic degradation of terbutylazine was investigated and obtained results are discussed. The structure of terbutylazine is presented on Figure 1. The Langmuir-Hinshelwood (L-H) mechanistic model is employed to describe the overall reaction rate.

2. Experimental set up

The photocatalyst employed was commercial titanium dioxide supplied by Degussa/Evonik (P25). The photocatalyst layer was prepared using chitosan [$[\beta$ -(1-4)-2-amino-2-deoxy-D-glucose] (Figure 1) for TiO_2 immobilization on glass fibre woven roving. Pure terbutylazine (99.6 %), an active ingredient of common herbicides, was chosen as a model component and obtained from a local producer Herbos d.d. Sisak. Terbutylazine belongs to the group of symmetrical triazine herbicides which are used extensively in agriculture and non-agricultural sites. The physico-chemical properties of the photocatalyst were investigated using Fourier transform infrared spectroscopy (FTIR) on the Bruker Vertex 70 with a diamond ATR sampling accessory and nitrogen absorption/desorption and powder X-ray diffraction (XRD) on a Shimadzu XRD 6000. The experiments were conducted in a batch reactor with recirculation, with an immobilized TiO_2 layer and equipped with a commercial 8 W UV-C lamp ($\lambda = 254 \text{ nm}$; $I = 12 \text{ mW cm}^{-2}$). Intensity of UV lamp, measured using a radiometer, did not change significantly during the experiments. A UV-A 8 W lamp ($\lambda = 365 \text{ nm}$) and a UV LED 7.2 W waterproof strip ($\lambda = 395 \text{ nm}$) were used for comparison to the UV-C germicidal lamp. The influence of various operating conditions, such as temperature, pH values, flow rate of recirculation, irradiation time was investigated. The source of irradiation was placed in the central part of the photoreactor. The reaction temperature was kept at selected temperature (25 – 70 °C) using a thermostat. Samples from the reactor were analysed using HP 1090 HPLC using a 5 μm , 250x4.6 mm SB-C18 column and a DAD detector.

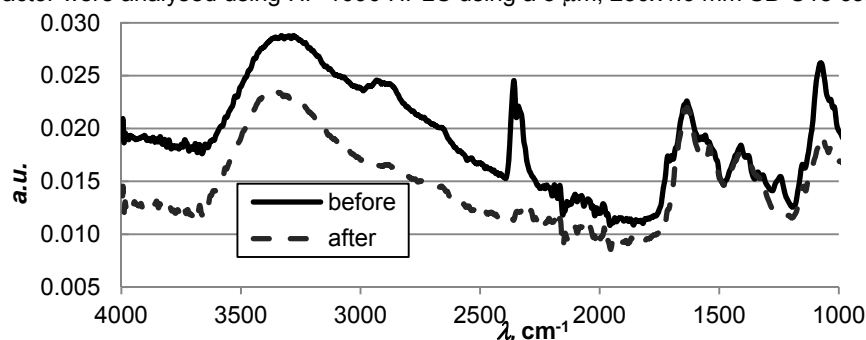


Figure 2. FT-IR analysis of the TiO_2 /chitosan photocatalyst before and after photocatalytic reaction in the reactor

3. Results and discussion

3.1 Investigation of the immobilized TiO₂/chitosan layer

FT-IR and XRD analysis were performed before and after the degradation experiments in order to determine changes in the two main components of the photocatalyst. The FT-IR analysis as presented on Figure 2 is used to determine whether chitosan goes through chemical transformation during the photocatalytic reactions, and the XRD analysis provides information of possible crystalline changes on the TiO₂ part of the photocatalyst. The peak at 2360 cm⁻¹ does not come from chitosan (Kasaai, 2008) and it cannot be from TiO₂, so it must be some impurity present in the catalyst that got washed out after. Other peaks show only smaller intensity, due to the dissolution of chitosan during degradation experiments, and no new peaks appeared after the reactions indicating that no chemical changes occurred on the chitosan molecule forming new bonds. The XRD analysis, as presented on Figure 3, confirms the dissolution of chitosan, the higher intensity of the major peak attributed to TiO₂ only occur due to the higher mass fraction of the semiconductor. The ratio of the peaks remains the same, showing an absence of crystalline transformations. The two peaks at 31.58 and 45.32 ° indicate the presence of NaCl used in the suspension, which dissolves during the final preparation step of the photocatalyst, which was confirmed by high concentration of Cl⁻ ions in the water used for conditioning.

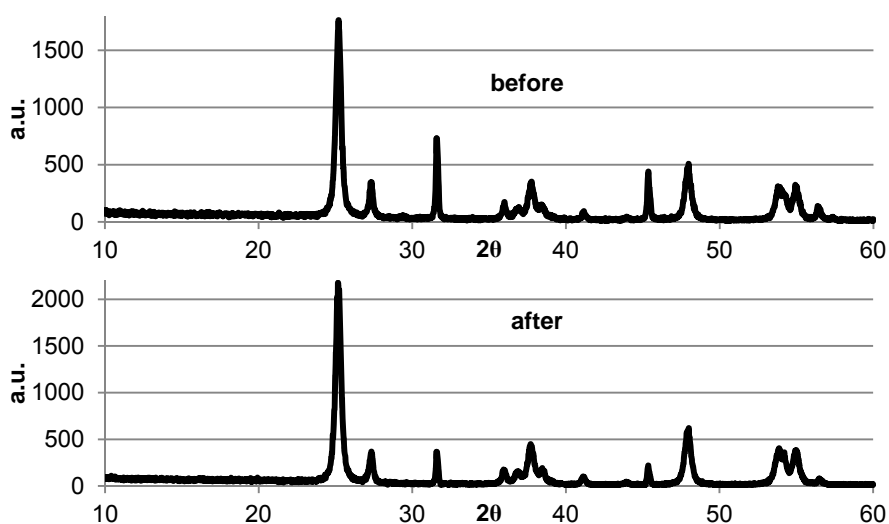


Figure 3. XRD analysis of the TiO₂/chitosan photocatalyst before and after photocatalytic reaction in the reactor

3.2 Degradation experiments

The photocatalytic activity of the prepared immobilized TiO₂/chitosan is evaluated by photodegradation of terbuthylazine (TBA) under UV light irradiation conditions and the results are compared to photolytic degradation under same conditions. TBA strongly absorbs UV light at 254 nm, and therefore photolytic degradation is expected. The results on the degradation part of TBA show that there are no major differences when photolytic degradation is compared to photocatalytic degradation (Figure 4). However the efficiency of the degradation reaction of terbuthylazine or other s-triazine herbicides is evaluated using the final product of the photolytic or photocatalytic reaction, cyanuric acid (Oh and Jenks, 2004). The evolution of the cyanuric acid (CYA) proves a different reaction pathway and a much bigger overall conversion to the final product in the presence of a source of hydroxyl radicals. The evolution of the cyanuric acid (CYA) proves a different reaction pathway and a much bigger overall conversion to the final product in the presence of a source of hydroxyl radicals. The different operating conditions were then evaluated for the photocatalytic reactions. Figure 5 shows the effect of the starting pH of the solution of the photocatalytic degradation of terbuthylazine (the initial concentration $c_{(TBA,0)}$) as well as the effect on the production of the desired product, the cyanuric acid. Due to the contribution of the photolytic degradation, there is no discernable difference in the degradation rate, the difference is only visible on the product. Under basic conditions, at pH 10.71, considerably lower concentrations of cyanuric acid are being created, while there is only a slight difference in its concentration when comparing neutral to acidic conditions.

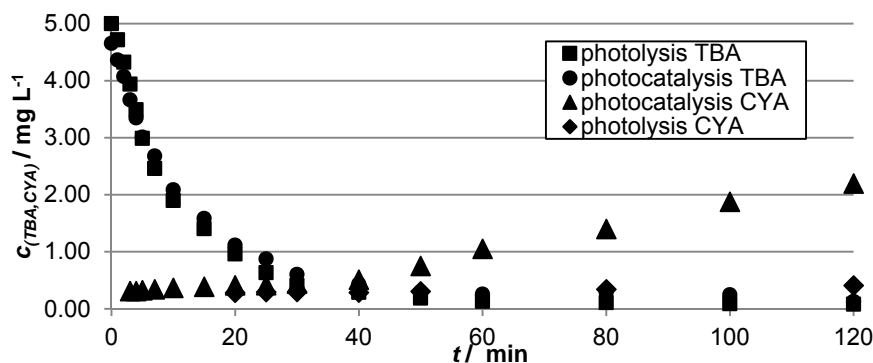


Figure 4. Comparison of photolytic and photocatalytic degradation of terbuthylazine and evolution of the cyanuric acid (Conditions: $C_{(TBA,0)} = 5 \text{ mg L}^{-1}$, $T = 25 \text{ }^\circ\text{C}$, $t = 120 \text{ min}$, $\lambda = 254 \text{ nm}$, $P = 8 \text{ W}$, $R = 300 \text{ mL min}^{-1}$, $\text{pH} = 5$)

The difference in the results can be explained by different effect of pH on the adsorption properties of the photocatalyst and the efficiency of the hydroxyl radicals formation. Since the pH of the terbuthylazine solution was between pH values of 5 and 6, there was no need to adjust the pH for the other experiments. The temperatures between 25 and 70 °C (Figure 6) were chosen according to the limits of the experimental system, knowing that we were using a glass reactor and rubber tubing, and the limits of industrial processes considering the cost and complexity of temperature regulation. Compared to other experiments the temperature does slightly affect the degradation regardless of the photolytic degradation rate, but the differences are again too small to be significant. The profile of the cyanuric effect, on the other hand, shows that temperature increases the overall degradation of the intermediate products of terbuthylazine. The profile of the cyanuric effect, on the other hand, shows that temperature increases the overall degradation of the intermediate products of terbuthylazine.

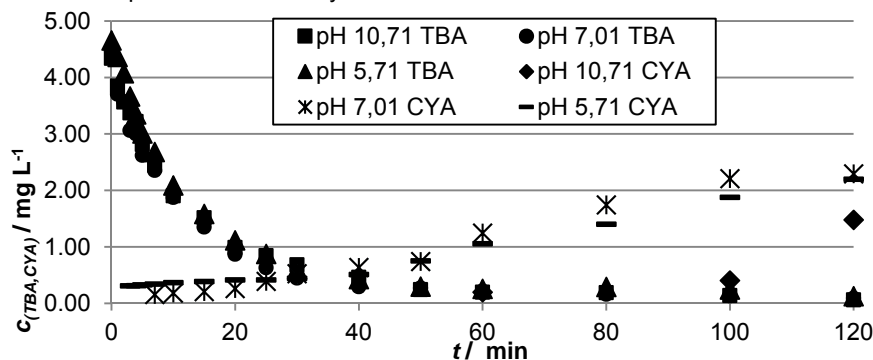


Figure 5. Photocatalytic degradation of terbuthylazine and evolution of cyanuric acid at different pH values (Conditions: $C_{(TBA,0)} = 5 \text{ mg L}^{-1}$, $T = 25 \text{ }^\circ\text{C}$, $t = 120 \text{ min}$, $\lambda = 254 \text{ nm}$, $P = 8 \text{ W}$, $R = 300 \text{ mL min}^{-1}$)

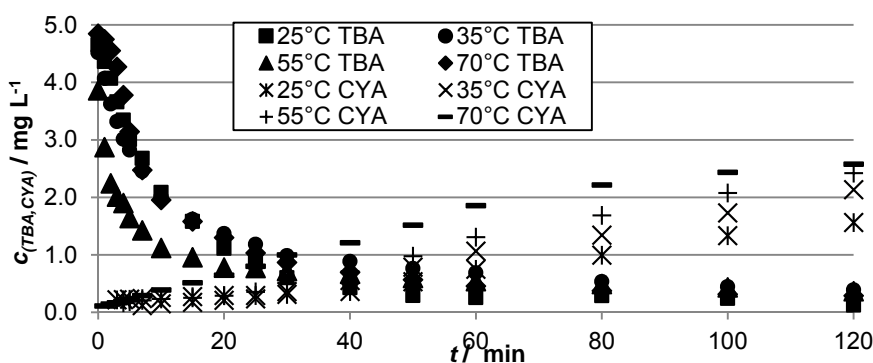


Figure 6. Photocatalytic degradation of terbuthylazine and evolution of cyanuric acid at different temperatures (Conditions: $C_{(TBA,0)} = 5 \text{ mg L}^{-1}$, $t = 120 \text{ min}$, $\lambda = 254 \text{ nm}$, $P = 8 \text{ W}$, $R = 300 \text{ mL min}^{-1}$, $\text{pH} = 5$)

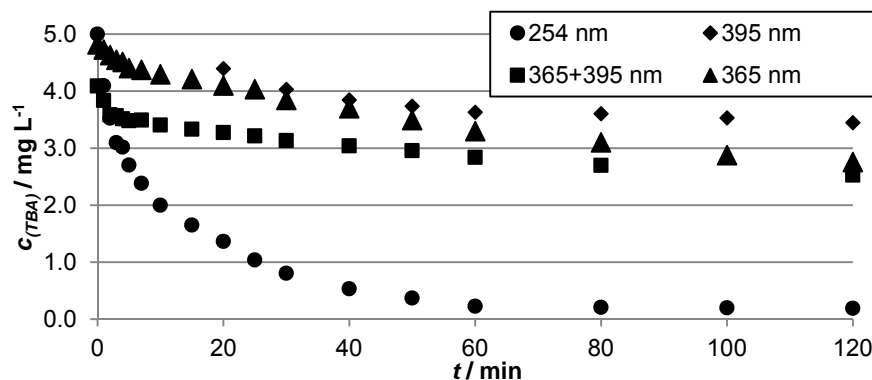


Figure 7. Photocatalytic degradation of terbuthylazine: ● 8 W 254 nm, ◆ a 7.2 W 395 nm LED strip placed close to the catalyst, ■ 8 W 360 nm lamp and 7.2 W 395 nm LED strip placed close to the catalyst ▲ 8 W 360 nm (Conditions: $c_{(TBA,0)} = 5 \text{ mg L}^{-1}$, $T = 25 \text{ }^\circ\text{C}$, $t = 120 \text{ min}$, $R = 300 \text{ mL min}^{-1}$, $\text{pH} = 5$)

The profile of the cyanuric effect, on the other hand, shows that temperature increases the overall degradation of the intermediate products of terbuthylazine. The increase in temperature negatively affects the adsorption properties of the photocatalyst, as well as the recombination speed of the semiconductor in the photocatalyst. Higher temperature also affect the solubility of oxygen in water, known to slow down the recombination speed of TiO_2 by absorbing electrons on the surface of the photocatalyst. Despite all that the degradation reaction rate at higher temperature compensates all those negative effects. Other radiation sources were tested to compare the overall degradation rate of terbuthylazine. Above 290 nm, degradation of terbuthylazine occurs only in the presence of the photocatalyst (Figure 7). The simplified Langmuir-Hinshelwood kinetic model was used to describe the photocatalytic degradation. This mathematical model is based on the supposition that the reaction occurs on the surface of the photocatalyst. The simple model used for this study uses the following assumptions of ideal mixing, negligible internal mass transfer resistance due to the very thin photocatalyst layer, isotherm conditions inside the reactor, time dependence of all variables inside the reactor and that the volume of the reaction solution is constant over time. The following reactor model (Eq. 1) can then be used:

$$r_A = f(C_{TBA}, T) = -\frac{dC_{TBA}}{dt} \quad (1)$$

This model can be used under the assumptions described above and considering that the chemical reaction can be described using a simple empirical kinetic model for a first order reaction (Eq. 2):

$$r_{TBA} = kC_{TBA} \quad (2)$$

The analytical solution is obtained combining both equations (Eq. 3):

$$kt = -\ln\left(\frac{C_{TBA}}{C_{TBA,0}}\right) \quad (3)$$

The example of the fit of the model for is given in Figure 8 representing the influence of temperature on the photocatalytic degradation of terbuthylazine. As it can be seen from the figure, the simple kinetic model is able to describe the main trend of the experimental data.

4. Conclusion

The objective of this study was to prepare a stable and robust photocatalyst for photocatalytic degradation of terbuthylazine. The catalyst was prepared using easily available materials proven to be also safe for the environment, resulting in a thin and stable layer of the $\text{TiO}_2/\text{chitosan}$ photocatalyst. Photolytic and photocatalytic degradation of terbuthylazine was performed to evaluate the contribution of the photocatalyst in degradation experiments at a wavelength below 290 nm, and to confirm the different reaction pathway. Photocatalytic degradation was performed under different operating conditions to find the optimal reaction conditions for photocatalytic degradation, the unaltered pH of the terbuthylazine solution proved to be effective enough and pH of the solution did not change more than 1 pH unit during all the reactions, proving a buffer

was not needed to control the reaction. Higher reaction temperature increases the degradation rate, but the temperature for a great number of experiments is limited by the actual reactor design and, for later use, by industrial operating conditions in water treatment plants. A simplified Langmuir-Hinshelwood kinetic model is able to describe the degradation of terbuthylazine (Figure 8), with more data available a more complex mechanistic model will be developed. Other radiation sources, more convenient for industrial application, were tested in comparison to the 254 nm lamp to be tested in subsequent research.

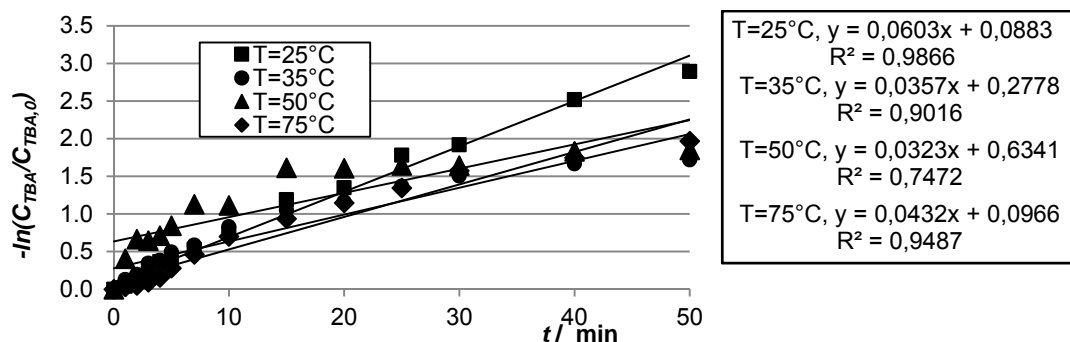


Figure 8. Photocatalytic degradation of terbuthylazine at different temperatures (■●▲◆ - experimental data, line – theoretical data, conditions: $c_{(TBA,0)} = 5 \text{ mg L}^{-1}$, $t = 120 \text{ min}$, $\lambda = 254 \text{ nm}$, $P = 8 \text{ W}$, $R = 300 \text{ mL min}^{-1}$, $\text{pH} = 5$)

References

- Ayati, A., Ahmadvpour, A., Bamoharram, F. F., Tanhaei, B., Mänttari, M. & Sillanpää, M. 2014. A review on catalytic applications of Au/TiO₂ nanoparticles in the removal of water pollutant. *Chemosphere*, 107, 163-174.
- Dash, M., Chiellini, F., Ottenbrite, R. M. & Chiellini, E. 2011. Chitosan—A versatile semi-synthetic polymer in biomedical applications. *Progress in Polymer Science*, 36, 981-1014.
- Dwight, D. W. 2000. 1.08 - Glass Fiber Reinforcements. In: ZWEBEN, A. K. (ed.) *Comprehensive Composite Materials*. Oxford: Pergamon.
- Ghimici, L. & Nichifor, M. 2013. Separation of TiO₂ particles from water and water/methanol mixtures by cationic dextran derivatives. *Carbohydrate Polymers*, 98, 1637-1643.
- Herrmann, J.-M. 2010. Photocatalysis fundamentals revisited to avoid several misconceptions. *Applied Catalysis B: Environmental*, 99, 461-468.
- Kasaai, M. R. 2008. A review of several reported procedures to determine the degree of N-acetylation for chitin and chitosan using infrared spectroscopy. *Carbohydrate Polymers*, 71, 497-508.
- Lin, C.-H., Lee, J.-W., Chang, C.-Y., Chang, Y.-J., Lee, Y.-C. & Hwa, M.-Y. 2010. Novel TiO₂ thin films/glass fiber photocatalytic reactors in the removal of bioaerosols. *Surface & Coatings Technology*, 205, 5341-5344.
- Mozia, S., Heciak, A., Darowna, D. & Morawski, A. W. 2012. A novel suspended/supported photoreactor design for photocatalytic decomposition of acetic acid with simultaneous production of useful hydrocarbons. *Journal of Photochemistry and Photobiology A: Chemistry*, 236, 48-53.
- Ormad, M. P., Miguel, N., Claver, A., Matesanz, J. M. & Ovelleiro, J. L. 2008. Pesticides removal in the process of drinking water production. *Chemosphere*, 71, 97-106.
- Tetzlaff, T. A. & Jenks, W. S. 1999. Stability of Cyanuric Acid to Photocatalytic Degradation. *Organic Letters*, 1, 463-465.
- Wilson, C. & Tisdell, C. 2001. Why farmers continue to use pesticides despite environmental, health and sustainability costs. *Ecological Economics*, 39, 449-462.